Hadronic showers in the PS data of FOCAL

Olivier Kesber

Supervisors:
prof. dr. T. Peitzmann
dr. ir. M. van Leeuwen

Utrecht University

Department of Physics
Institute of Subatomic Physics

January 17, 2017

Abstract

In this bachelor research, the data taken by the FOCAL prototype at the Proton Synchotron beam is analysed, to study characteristics of the hadronic showers and compare the characteristics to simulations done with the GEANT 4 software package. These hadronic showers are induced by protons and pions. In this research an event by event approach is used to study the characteristics and correlation between different experimental values is calculated to separate the different types of hadronic showers.

Contents

1 Introduction

This bachelor research is done at the Institute of particle physics of the Utrecht University in the FOCAL (forward calorimeter) group. This research group is working on the development of a new calorimeter for the next large-scale upgrade of ALICE at CERN. At the time of the research, the group had developed a prototype based on digital high-resolution silicon chips and Tungsten absorber. This prototype was tested at CERN in September 2014. The data collected at that test is analysed in this thesis.

2 Theoretical background

2.1 Passage of particles in matter

When particles travel through matter they interact with the medium in different ways. This depends on the incoming particle as well on the medium. This section will focus on how different particles will react with matter.

2.1.1 Heavy charged particles

Heavy particles with charge interact mainly with the electrons of the absorber material (through Coulomb interactions). There are two possibilities, the first one is excitation and the other one is ionisation. Excitation means that the electron of the absorber is lifted to a higher energy level. The other possibility is that an electron of the absorber is ejected from the atom This effect is dominant when the energy of the incoming particle is larger than the atomic binding energy. The energy loss due to ionisation is approximated by the Bethe-Bloch formula: [1]

$$-\frac{dE}{dx} = Z^2 \frac{4\pi n z^2 e^4}{m_e v^2}\left[\log\left(\frac{2m_e v^2}{I(1-(v/c)^2)}\right) - \left(\frac{v}{c}\right)^2\right] \tag{1}$$

Here dE is the energy lost in a distance dx, n is the number of electrons per cm^3 and Z is the atomic number of the absorber, m_e is the electron mass v is the speed of the particle and I is the mean excitation potential of the absorber. Heavy charged hadrons can also interact trough the strong force this is further explained in subsection 2.1.4.

2.1.2 Light charged particles

Light charged particles can interact like heavy charged particles but they can also lose energy through radiation. These different interactions are dominant in different energy regions and these regions are separated by the critical energy. The critical energy for solids is: [2]

$$E_{\mathrm{c}} \approx \frac{610\mathrm{MeV}}{Z + 1.24} \tag{2}$$

In the region where $E < E_\mathrm{c}$ light charged particles interact very similar to heavy charged particles. In the region where $E > E_\mathrm{c}$ two interactions are possible, Coulomb scattering or the deflection of incoming particles or Bremsstrahlung what occurs when a charged particle scatters in the coulomb field of absorbers atom. The energy loss in this process scales with $\frac{E}{(mc^2)^4}$ .That is why is effect is small for particles with higher mass.

2.1.3 Photons

A photon interacts in three different ways with the absorber. The first one is the photoelectric effect. In this process an atom absorbs a photon and emits an electron, this is dominant at energies below 10 keV. The second is the Compton effect or Compton scattering, a photon scatters off a free electron. Last is pair production. Here a photon decays into an electron-positron pair. This is possible at energies $> 2m_ec^2$.

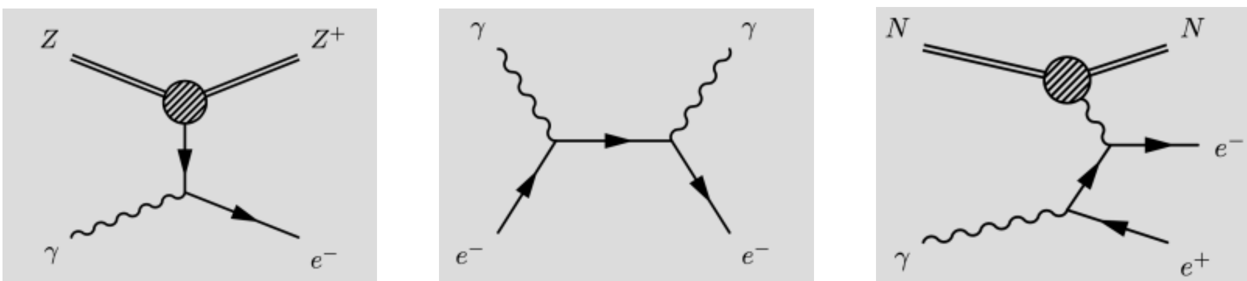

(a) Ionisation (b) Compton scattering (c) Pair Production

Figure 1: Photon interactions

2.1.4 Neutral particles

The interactions mentioned above are all electro-magnetic so a neutral particle will not undergo such reactions. But neutral hadrons can interact through the strong force with the absorber. The odds that a reaction like this happens is very small due to the short range of the strong force.

2.2 Shower

If a highly energetic particle enters a medium it can interact (as described in section 1.1), but if the energy of the incoming particles is high enough that the produced particles again can interact with the medium a shower can be produced (by this definition a cascade would be a better name for it). In calorimetry, a shower in a certain material is used to measure the energy of the incoming particle.

2.2.1 EM shower

We define a shower to be electromagnetic if the particle that comes in is either an electron or positron or a muon. These particles can not interact with the absorber through the strong nuclear force and therefore they can only interact electromagnetically with the absorber. possible effects are: excitation, ionisation and radiation effects.

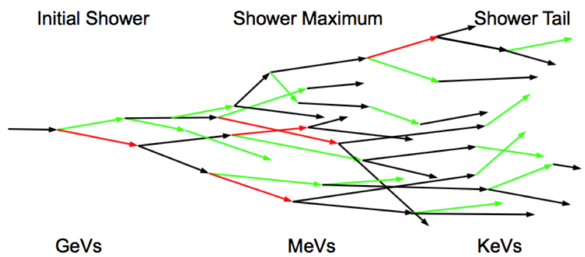

Figure 2: schematic view of a shower

2.2.2 Hadronic shower

The definition of a hadronic shower is that the incoming particle is a hadron. In this thesis, the two main hadrons are protons and pions. The big difference between an EM shower and a hadronic is that the "heavy" hadrons can't produce radiation like an electron but they can ionise the absorber. On the other hand, a incoming hadron can interact with the nucleus of the absorber through the strong interaction. In a strong interaction, a lot of different things can happen. One of the possibilities is the creation of a neutral pion. These decay into photons which will interact only electromagnetically.

So a hadronic shower can have an electromagnetic part and a hadronic part. Because there are so many different possible reactions in a hadronic shower is it hard to effectively describe them. But there are some variables which can be parametrized. The first is the shower maximum.[8]

$$L_{\text{max}} \approx \lambda(0.6\log(E - 0.2)) \tag{3}$$

Here λ is the interaction length which is explained in section 2.3 and the E is the energy of the incoming particle in GeV. The longitudinal containment of 95 % of the shower in other words shower depth is approximated by:[8]

$$L_{\text{containment}} \approx L_{\text{max}} + 4\lambda(E^{0.15}) \tag{4}$$

Again the energy E is in GeV. The radial containment of 95 % of the shower can be approximated by:[8]

$$R_{\text{containment}} \approx \lambda \tag{5}$$

2.3 Interaction length and depth

Interaction length is the mean distance travelled by a particle before undergoing a strong interaction. It can be approximated by a classical mean free path approach. The cross section for the interaction between a proton and a nucleus is approximated by:[9]

$$\sigma \approx 4 \times 10^{-26} (A)^{2/3} \mathrm{cm}^2 \tag{6}$$

where A is the atomic mass number of the nucleus. Then the mean free path is:[9]

$$\lambda = \frac{1}{N\sigma} \approx \frac{A^{1/3}}{\rho} \frac{1}{N_A 4 * 10^{-26}} \approx \frac{A^{1/3}}{\rho} 35 \text{ g cm}^{-2} \tag{7}$$

here N_A is the Avogadro number and N is the number of scatter centers per unit volume which is equal to $\rho\frac{N_A}{A}$

2.4 Radiation length X_0

The radiation length is the distance over which the energy of a particle is reduced to $1/e$ (37%) of its original energy. It is approximated by:[3]

$$X_0 \approx \frac{1432.8A}{Z(Z+1)(11.319 - \log(Z))} \text{g cm}^{-2} \tag{8}$$

Where Z is the atomic number and A is the mass number. The radiation length of a material with different compounds is given by:

$$X_{tot} = \left(\sum_{i=1} \frac{V_i}{X_i} \right)^{-1} \tag{9}$$

2.5 Moliere radius

The Moliere radius is the radius of the cylinder that contains on average 90% of the deposited energy of an electromagnetic shower and 99% within 3.5 radii. This is used to describe the lateral development of the shower. The Moliere radius can be calculated by: [2]

$$R_{\mathrm{M}} = E_{\mathrm{s}} \frac{X_0}{E_{\mathrm{c}}} \tag{10}$$

Where E_{s} is defined as $m_{\mathrm{s}} c^2 \sqrt{\frac{4\pi}{\alpha}}$. The Moliere radius is a useful number in calorimetry because it determines the capacity (of a calorimeter) for separating showers in a volume. Another interesting thing about Moliere radius is that it does not depend strongly on the Z of the material. Because X_0 scales with $\frac{A}{Z^2}$ and with most elements the ratio A to Z lies close to one (within first order approximation), so Z scales with Z^{-1} to first order. E_{c} also scales with Z^{-1}. The Moliere radius is the ratio between the two, so the Z dependence cancels out to first order.

3 Experimental setup

3.1 Accelerator & beamline

The data that is used for this thesis was taken at the test facilities at CERN and the beam that is used is accelerated in the Proton Synchrotron (PS).

The Proton Synchrotron is a particle accelerator at CERN, containing 277 conventional electromagnets including 100 dipoles (that are used to bend the beam). This leads to a maximum energy of 25 GeV. It first collided protons on 24 November 1959. Today it has multiple duties. The first is to accelerate protons coming out the Proton Synchrotron Booster or heavy ions from Low Energy Ion Ring (LEIR) and deliver the particles to more powerful and bigger accelerators. The other job is that of feeding the accelerated particles directly to the east area where it is used for different kinds of experiments. The test beam used for this research consists of secondary particles of accelerated protons. The beam-composition is dependent on production angle and its momentum is determined by a combination of dipoles, quadrupoles and collimators. That is why the beam-composition is never purely one type of particle but always a mixture of different types of particles. There are also muons flying through the collimators and other protecting material but these are neglected in the measurements. At the energies used for this research (10 and 8 GeV), the beam consist of mostly protons and pions [5]. The PS is used because it can produce a beam with energy lower than 10 GeV, Another advantage of the PS is that is it easier to get test beam time than at the larger accelerators.

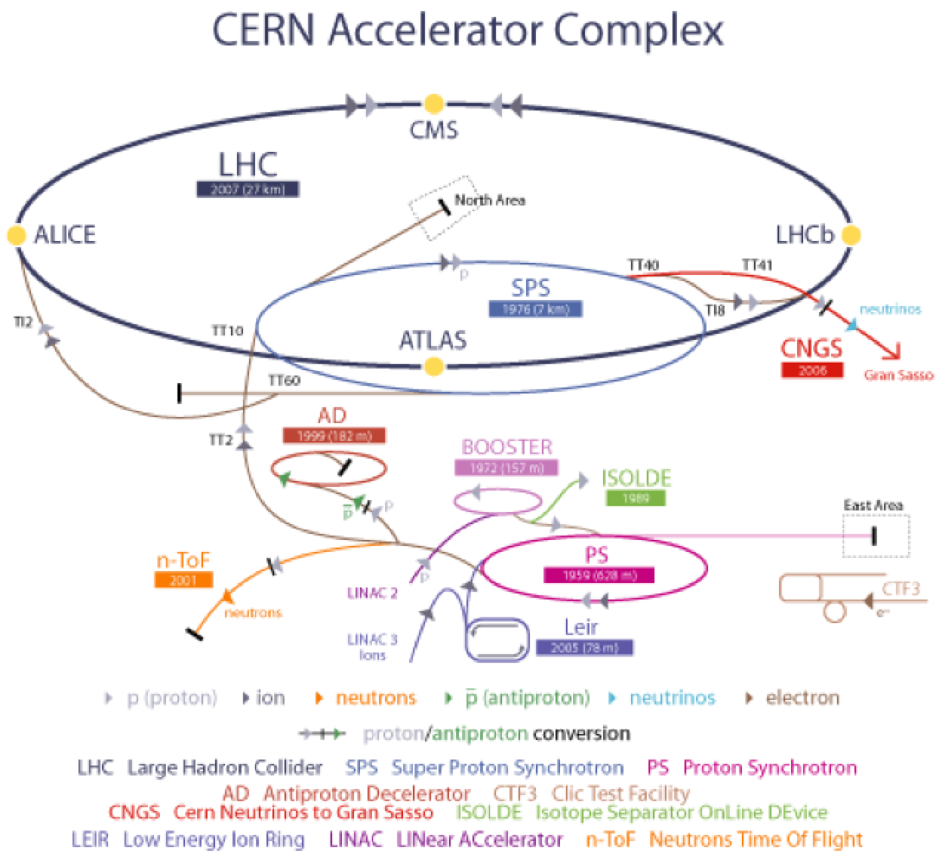

Figure 3: Schematic diagram CERN-Accelerators-Complex

3.2 The detector

The test of the detector prototype is done in the T9 area of the East Hall at CERN (shown in figure 5). In the test setup 2 Cherenkov detectors, 5 scintillators and the FOCAL detector itself are used. A schematic view of the detector and the scintillators is shown in figure 4.

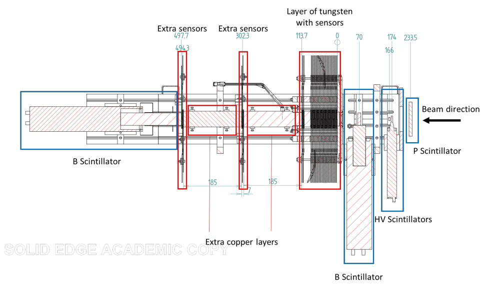

(a) Top view

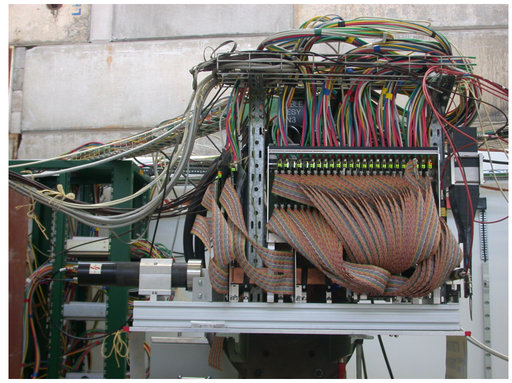

(b) Side view

Figure 4: Schematic diagram and photograph of the detector [11]

Figure 5: A map of the East Hall at cern

3.2.1 Absorber

In the PS setting the FOCAL prototype has a thin layer of aluminium in front. Between each two chips is a layer of tungsten (of circa one X_0) and between the last three sensors are two copper blocks. The choice of absorber is based on four properties: high density, short radiation length, small Moliere radius and high thermal conductivity. The high density, short radiation length and small Moliere radius are needed to minimise the physical size of the detector. A high thermal conductivity is needed cool the heat generating sensors. Tungsten matches all these criteria as shown in table 1. The last two layers of absorber are added to optimise the containment of hadronic showers. Copper is used because the ratio of radiation and interaction length is better for the containment of hadronic showers and it is easier to work with than tungsten.

Table 1: Properties of tungsten and copper[2]

Material	ρ (cm^2)	X_0	R_M	λ
W	19.3	0.3504	0.9327	173
Cu	8.96	1.436	1.568	400

The full layout of the detector is given in the appendix.

3.2.2 Maps chips

Between the layers of tungsten, the sensors-layers are placed. There are 24 (sensor)layers and each layer consists of 4 MAPS chips. MAPS stand for a Monolithic Active Pixel Sensor. These chips are build up out of CMOS structures. So if a particle passes trough the chips, it will deposit charge, that charge is then stored in an n-well. The chips can only capture the charge but not measure it. To measure the charge in the pixels a rolling read-out method is used. This method has an upside that it needs 640 times fewer discriminators than a conventional method. On the other hand, the downside of the method is that the readout time is relatively long (642μs). A result of this type of detector is that the detector measures particles but does not measure their energy. So the signal produced by the detector scales with the number of particles in a shower. This is rather unique because classical detectors (analogue) measure the energy deposition of particles. To collect the information from the extra layer (between the copper blocks) layer 19 and 21 are unplugged and the layers 24 and 25 are plugged in.

3.2.3 auxiliary detectors

Scintillator The scintillators consist out of two components. The first one is a piece of scintillating material and the second one is a photo-multiplier tube. Most common scintillating material are kinds of plastics. In these plastics an electron is excited by an incoming particle and when the electron falls back to its ground state it emits a photon. The direction of the emitted photon is completely random so does not depended on the direction of the incoming particle. So some photons will be emitted in the direction of the photomultiplier tube. A photomultiplier tube works by converting the incoming photon into an electron with a photo-cathode. This electron is directed into an electron multiplier where the electron is multiplied by a number of dynodes with different potential. After the dynodes, there is an

Table 2: Different scintillators with size and place

Label	Size (cm)	Place
F	4x4	Front
P	11x11	Front
H	4x1	Front
V	1x2	Front
B	4x4	Back

anode which converts the incoming electrons to a sharp current pulse which can be detected. This process is shown in figure 6. The different scintillators with there size are given in table 2.

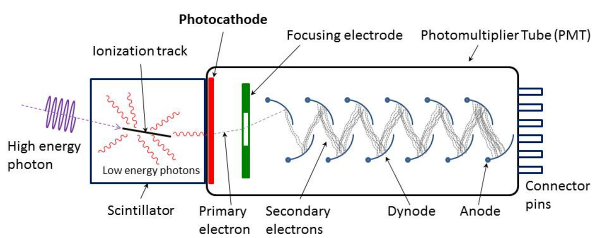

Figure 6: Schematic diagram of a photomultiplier tube coupled to a scintillator.[4]

Cherenkov detector A Cherenkov detector is a detector that uses the Cherenkov radiation to determine the velocity of an incoming particle. Because the momentum of the incoming particles is known the mass of the incoming particle can be determined. Cherenkov radiation comes from the fact that particles in a dielectric medium can have a velocity higher than the phase velocity of light in that medium. When a particle moves through the dielectric material it will excite electrons to a higher orbit, when the electron falls back again it will emit a photon. In the special case that the particle is moving through the media faster than the phase velocity of light in that medium, the produced photons will interfere with other photons. This process can be compared to a sonic boom of sound waves. In a Cherenkov detector, the produced photons are detected by a photomultiplier to produce a signal. In this set-up a gas chamber is used as the medium, the pressure of this gas was set 0.5 bar. This is done to discriminate protons and pions.

4 Data selection

4.1 Triggerbits

To determine if a particle comes in and what the incoming particle is the auxiliary detectors are used. The information provided by these auxiliary detectors is stored in a bit which is called a triggerbit. The set-up as used for the PS beam test makes use of 5 different scintillators and two Cherenkov detectors.

4.1.1 Scintillators

The scintillators are used to provide information on when and where a particle comes in. This is done by combining the signals from the different scintillators. An incoming particle that enters the detector will be detected by the P and the F scintillator so if both scintillators give a signal at the same moment there is a particle entering the detector. If a particle makes it all the way through the detector it will produce a signal from the B scintillator so again if the B scintillator and the F scintillator give a signal at the same time a particle went in and all the way to the end of the detector. If a particle comes in at the centre of the detector it will hit the cross section of the Horizontal and Vertical scintillator so if both give a signal at the same time a particle entered the detector at the centre $1cm^2$. These combinations (table 3) are the triggers for the detector.

4.1.2 Cherenkov detector

To determine what kind of particle is coming in two Cherenkov detectors are used. If both of them give a signal the incoming particle is a pion and if the Cherenkov doesn't give a trigger, the incoming particle is a proton.

Table 3: Triggers and the function of the triggers

Trigger	Function
Cherenkov(CF)	Incoming particle is a pion
Front scintillator(PF)	Particle at the front of the detector
Central scintillator(HVF)	Incoming particle at the centre of the detector
Back scintillator (BF)	Particle at the back of the detector

4.2 Selection

To select the interesting events it is necessary to look at coincidental of the triggers.

Table 4: Number of triggers for different combinations

Combination of triggers	Number of events 8 GeV/c	Number of events 10 GeV/c
HVF	542	905
HVF and BF	192	211
HVF and CF	102	103
HVF and notCF	440	802
HVF and BF and CF	73	78
HVF and BF and notCF	119	133

An interesting value is the one of the HVF and BF triggers in comparison with the number of enents with a HVF trigger, this one should count all the events where the outgoing particle has enough energy to produce a signal in the B scintillator. So you would expect a higher number of events that match this criterion's because almost all the hadrons will not lose all their energy within the detector. This could indicate that the B scintillator is not optimal calibrated or there is significant leakage trough the sides of the detector.

4.3 Past-future protection

Because the detector makes use of the rolling readout method it can happen that two triggers are measured shortly after each other. When is happens it could be possible that there are two particles in the detector. This is called pile up. To correct for this, a past and future protection method is used [6]. This is a method of only selecting events where there are no other triggers are close in time.

5 Experimental showers

The experimental data is processed and analysed with the root software package, complemented with the macro's of M. Reicher, H. Wang and C. Zhang.

5.1 Raw signal

One of the easiest ways to output the experimental data is by making a hit map. A hit map is a plot where all the pixels in one layer that give a signal are plotted and all those plots are overlaid on top of each other as shown in figure 7.

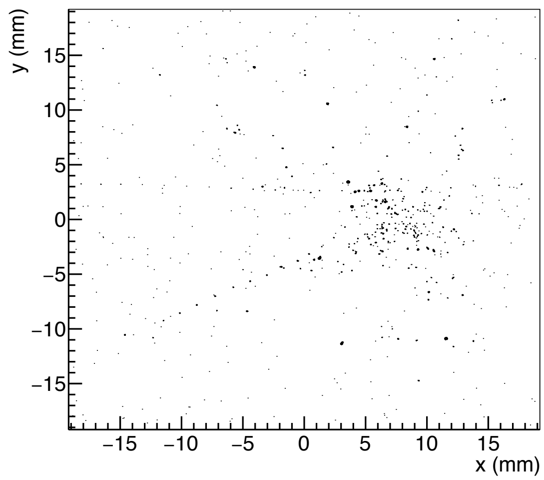

Figure 7: Hit map of a 10 GeV/c proton

A similar plot is the hit map projected on the x-axes (or y) and the depth axes.

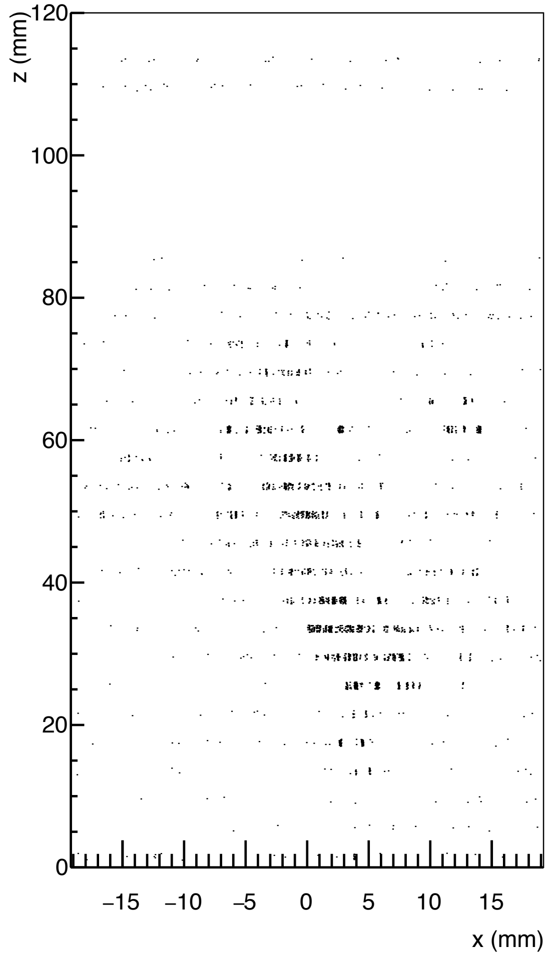

Figure 8: Hit map (XZ) of a 10 GeV/c proton with x and z in mm, N.B. axis are scaled

5.2 Hit distribution

To analyse the full data set it is interesting to look at the hit distributions. This is a plot that has total number of hit on the x axes and number of occurrence on the y-axes.

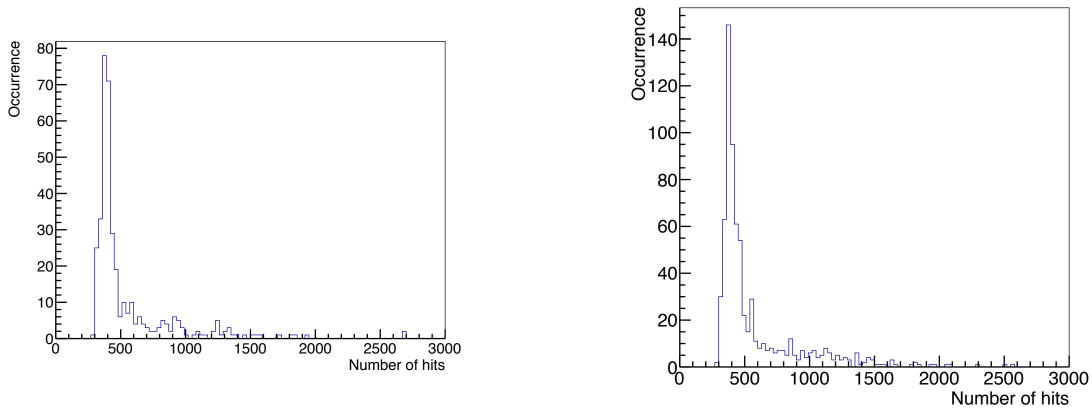

Figure 9: Hit distribution of protons with total number of hit on the x axes and number of occurrence on the y-axes. Left 8 GeV/c and right 10 GeV/c

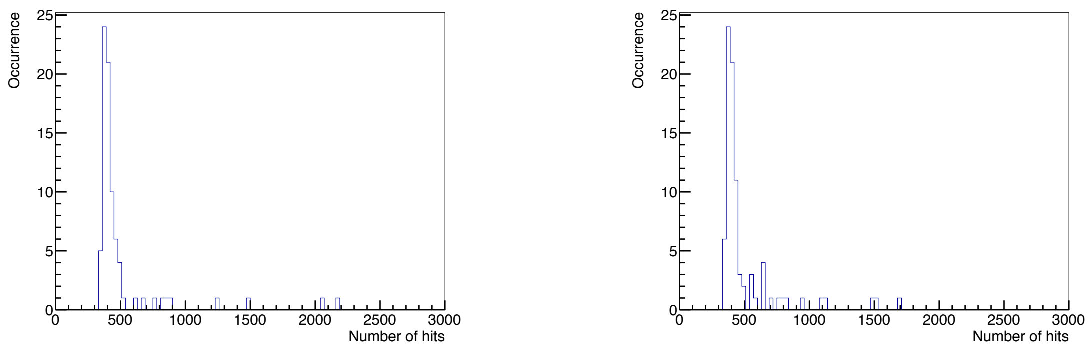

Figure 10: Hit distribution of pions with total number of hit on the x axes and number of occurrence on the y-axes. Left 8 GeV/c and right 10 GeV/c

5.3 Event by event analysis

It is interesting to look at the characteristics of single showers and try to discriminate between the different types of hadronic showers. Most of these characteristics of single hadronic showers are calculated from the longitudinal profile of one event. An example of a longitudinal profile is shown in figure 11.

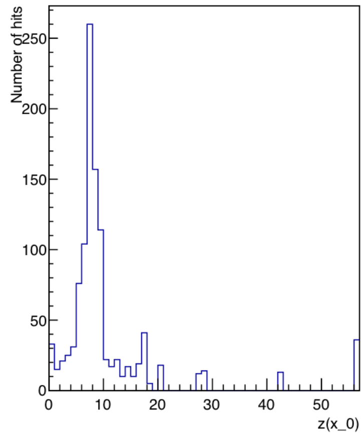

Figure 11: Longitudinal profile of a single 10 GeV/c proton The z-coordinate is expressed in units of radiation length.

5.3.1 Longitudinal profile

The longitudinal profile contains a lot of information about one event. The type of event is easily seen in the longitudinal profile. So, for example, the a track (particle passing through without starting a shower) will have an overall low number of hits, while a particle that starts a shower will have a longitudinal profile with a larger number of hits as in figure 11.

5.3.2 Shower characteristics

Several shower characteristics are calculated from the longitudinal profile. Here a new variable is introduced t is a place in the detector defined as: $t = \frac{z}{X_0}$ (so it has the same dimensions as radiation length). The first one is the start point. A start layer is defined as the first layer where the number of hits is larger than 45 and the next layer has also more than 45 hits or the layer after that second layer has more than 45 hits. This option to "skip" a layer is used because in some layers some chips are malfunctioning. This effect should not affect the determination of the start point. The value of 45 is chosen because the noise level is around 25 and typical showers have more than 45 hits per layer. The second one is the end point of the shower. The end point is defined such that the last layer of the shower has more than 45 hits but the next four layers measure values less than 45 hits, then the endpoint is defined as the first layer in which the number of hits is less than 45. It is clear that the end and start layer are not defined in a symmetric way. This is because of the bad layers that also affect the determination of end layers. With the information of the start- and endpoint, the length of the shower is easily calculated by subtracting the place of start-piont from the place of start-piont. Other interesting values are the maximum number of hits in one layer and the total number of hits within the shower (between start and end point).

Table 5: Definition of shower characteristics

Characteristics	definition (Hit(i)= number of hits in layer i))
start point (t_{start})	(Hit($i > 45$) &(Hit($i+1 > 45$) or Hit($i+2 > 45$)) then $t_{start} = i-1$
End point (t_{end})	Hit(i) > 45 & Hit($i+1$) < 45&Hit($i+2$) < 45 & Hit($i+3$) < 45 &Hit($i+4$) < 45 then $t_{\text{end}} = i+1$
Length of the shower (Δt)	$\Delta t = t_{\text{end}} - t_{\text{start}}$
Total number of hits (N_{tot})	$N_{\text{tot}} \sum_{i=t_{\text{start}}}^{t_{\text{end}}} \text{Hit}(i)$
Maximum number of hits in one layer (N_{max})	N_{max} =Max value of Hit(i) between t_{start} and t_{end}

6 Simulation

To simulate the hadronic showers the software package GEANT 4 is used. In each simulation 1000 incoming particles are distributed over the central one square centimetre of the detector. The virtual detector used in the simulation is identical to the real one (including the dead chips) with the difference that all the chips have the same sensitivity, so no calibration is needed with simulation data. But it is possible to simulate an event as if it was in a detector without dead chips. This is called a perfect detector simulation.

6.1 Charge sharing threshold

To proper simulate a hadronic shower the correct threshold for charge sharing should be set. This is a variable that set a boundary on how and when charge spreads out in the process of a (hadronic) shower. The best way to determine the best value for the charge sharing threshold is by statistically analyse the difference between the experimental hit distribution and the simulated hit distribution and minimise the difference.

6.2 Hit distribution

The hit distribution of the simulated data is calculated in the same manner as with the experimental data.

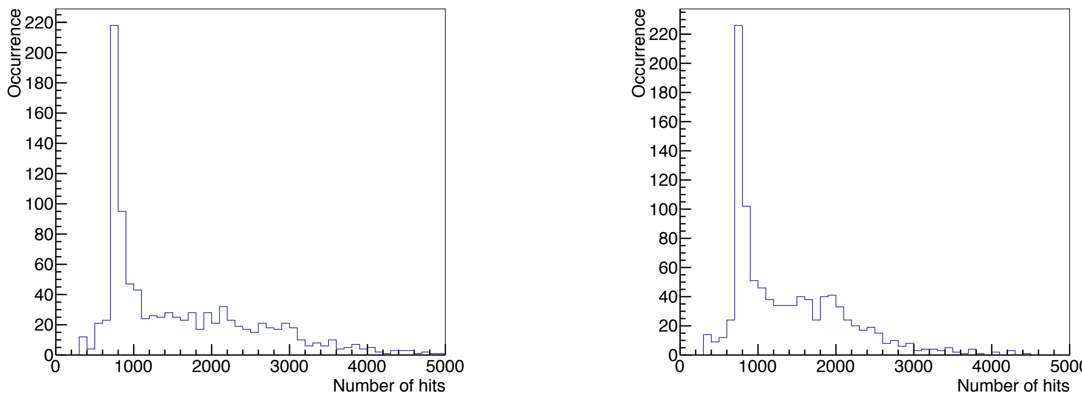

Figure 12: Simulated hit distribution of Protons left 8 GeV/c and right 10 GeV/c

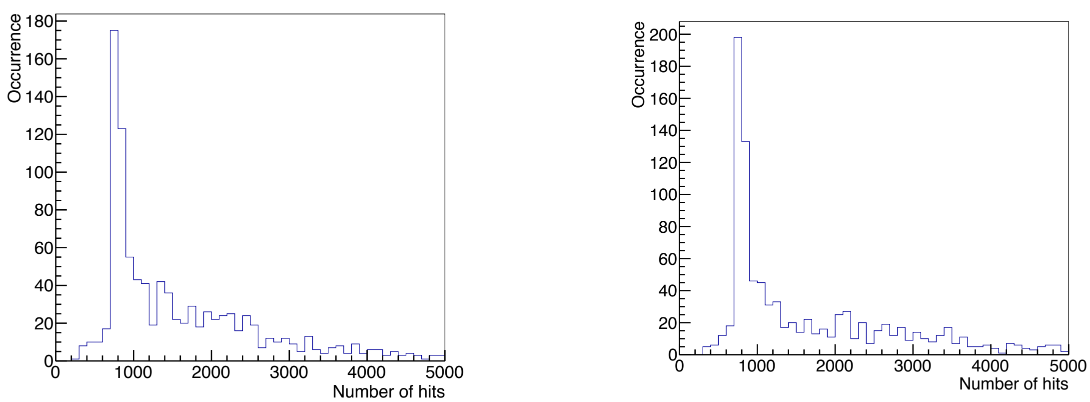

Figure 13: Simulated hit distribution of pions left 8 GeV/c and right 10 GeV/c

Figure 12 and 13 shows two unexpected results. The first one is the presence of events with more than 4000 hits and the other one is that the peak is at 700 hits. The maximum number of hits in an electromagnetic shower is 2111 for 8 GeV/c and 2657 for 10 GeV/c (with an error of $\sqrt{n}$)[10]. It is not expected that a hadronic shower would have a higher maximum number of hits than the electromagnetic shower. The peak is expected to be around 375 same as in the experimental data (figure 9 and 10).

6.2.1 Longitudinal profile

The longitudinal profile of the simulated showers is shown in figure 14 and 15. The shape of this profile is not very smooth en therefor impossible to calculate start point and end points the same way as done for the experimental data.

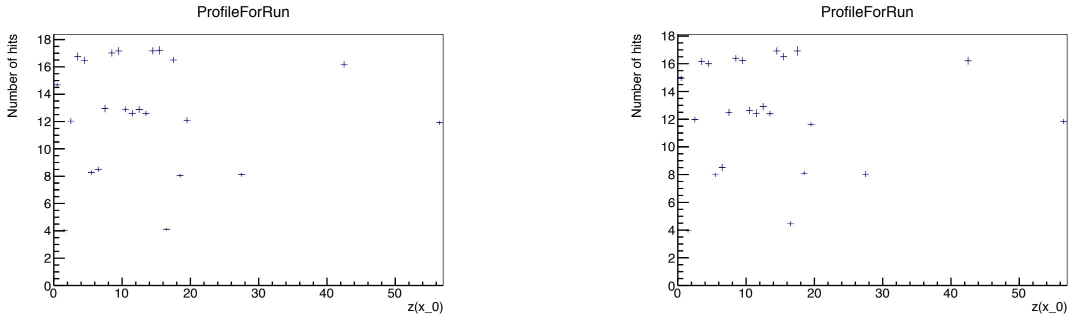

Figure 14: Simulated longitudinal profile of Protons left 8 GeV/c and right 10 GeV/c

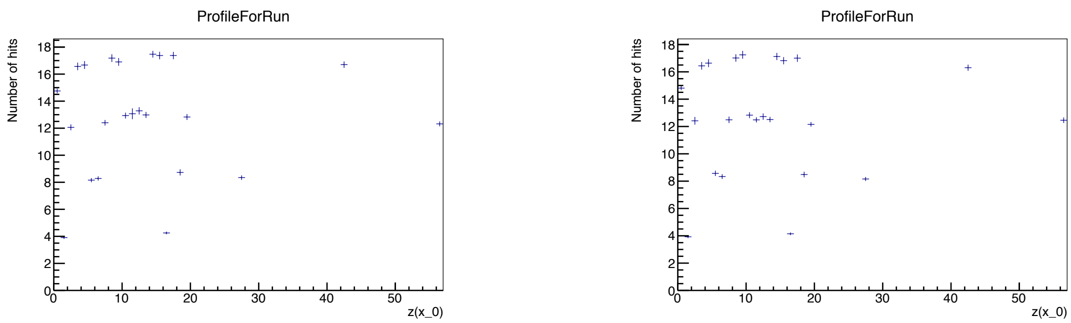

Figure 15: Simulated longitudinal profile of pions left 8 GeV/c and right 10 GeV/c

7 Results

In this chapter, the characteristics (start point of the shower, the end point of the shower and length of the shower and the correlations between length, the total number of hits, maximum number of hits in one layer) will be calculated from the experimental data. To calculated the characteristics of the showers it is important to use only those events that have a well-defined start point and a well-defined end point. With this constrain the data sample reduces even further. But it is necessary because all characteristics should be calculated from the same data sample.

7.1 start-point

The start point of the shower is an interesting value because at 8 and 10 GeV/c it will most likely be a strong interaction between the incoming particle and a nucleus of the absorber. Another advantage of the quantity start point is: that it is well defined (other definitions of start points are very similar).

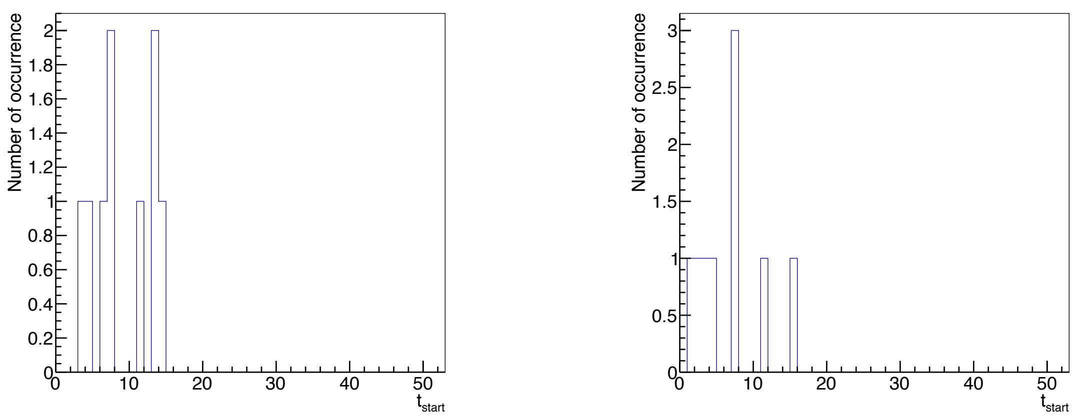

Figure 16: Start-point of pions left 8 GeV/c and right 10 GeV/c

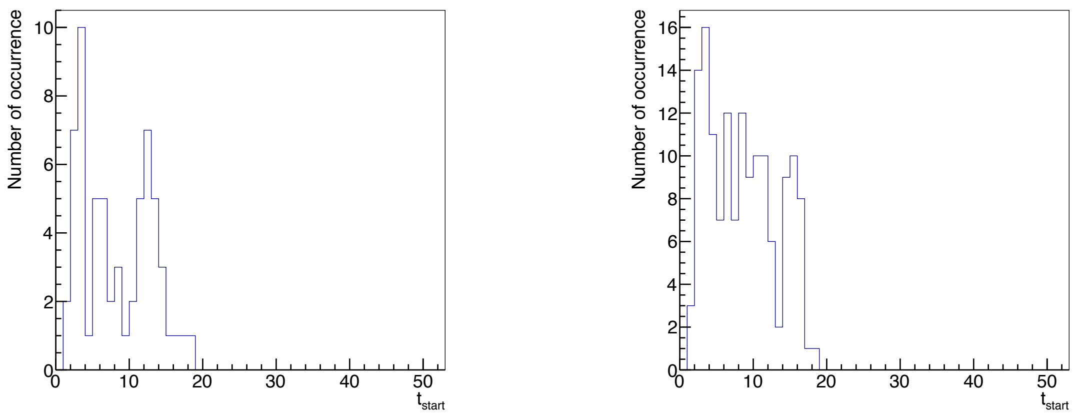

Figure 17: Start-point of Proton left 8 GeV/c and right 10 GeV/c

This result of the 8 GeV/c protons shows that there are two regions where most showers start, something that is not expected from the theory. The 10 GeV/c protons show a better profile for the start point of the shower. Because we would expect that all layers have roughly the same probability of starting a shower. This is so because it the interaction probability is an exponential function and it is expected that it would show as the tail of the function.

7.2 Endpoint

The end point is also an important quantity to calculate but it can be defined in different ways what will lead to different results. This calculation is based on the definition stated in table 5 and only events that have a start point are used to calculate end points.

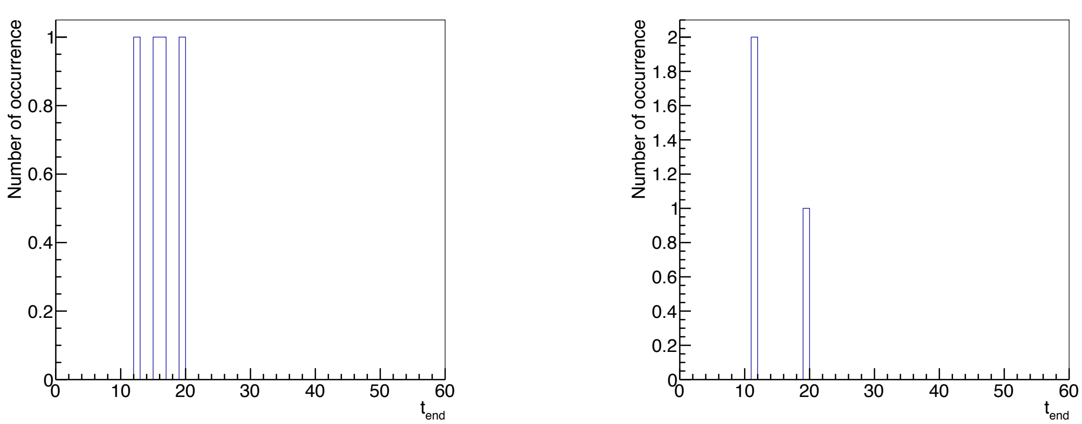

Figure 18: Endpoint of pions left 8 GeV/c and right 10 GeV/c

The first thing that shows up is the low total number of end points. This is because for some events it is not possible to define an end point. Because of this low statistic, it is not interesting to calculate other characteristics for the pion showers.

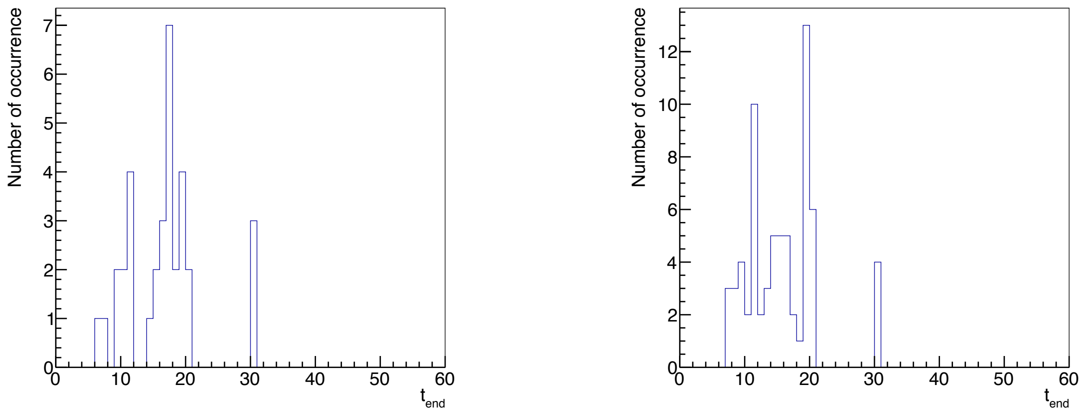

Figure 19: Endpoint of Proton left 8 GeV/c and right 10 GeV/c

Because there are a lot of possibilities for a hadron shower there are a lot of possibilities for the development of the different showers. So the random profile is shown in figure 19 is expected.

7.3 Length

The length (Δ t) build up out of the start point and the end point of the shower and so the argument that holds for the end point also holds for the length. The profile of length of the shower depends on the definition of the end point.

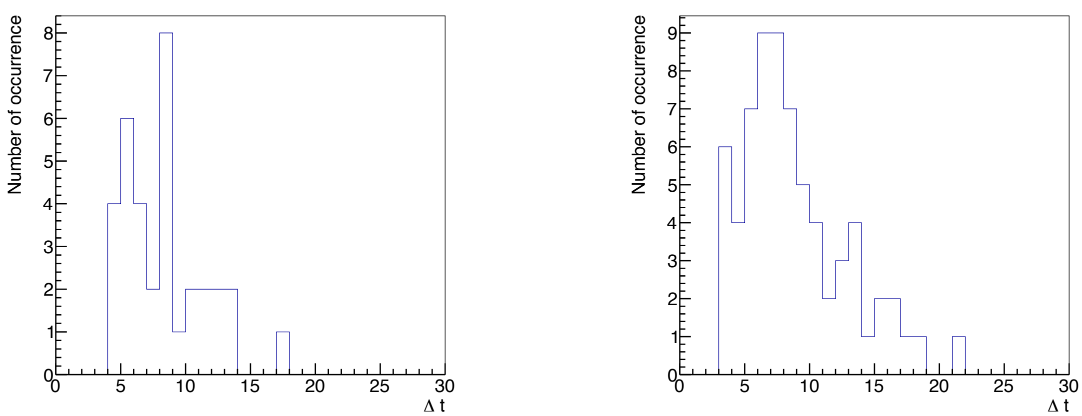

Figure 20: Length of Proton left 8 GeV/c and right 10 GeV/c

Interesting about this result is that in both energies there is a peak around a length of Δt = 7. This may indicate that there is a type of hadronic shower that (with this definition of start and end point) has a length of roughly 7 radiation lengths. The rest of the distribution looks like expected because the length of a shower is a combination of start point and end point of the shower more showers with a short length are expected then showers with a long length.

7.4 Correlations

The quantities length N_{max} and N_{total} (defined in table 5) can be used to calculate correlations that could give information about the characteristics of the different types of hadronic showers. Because the energy dependence of these quantities is low the plots in this section show events of 8 and 10 GeV/c protons.

7.4.1 Total vs max

The correlations between the total number of hits (x-axis) in the shower and the maximum number of hits in one layer (y-axis) is shown in figure 21.

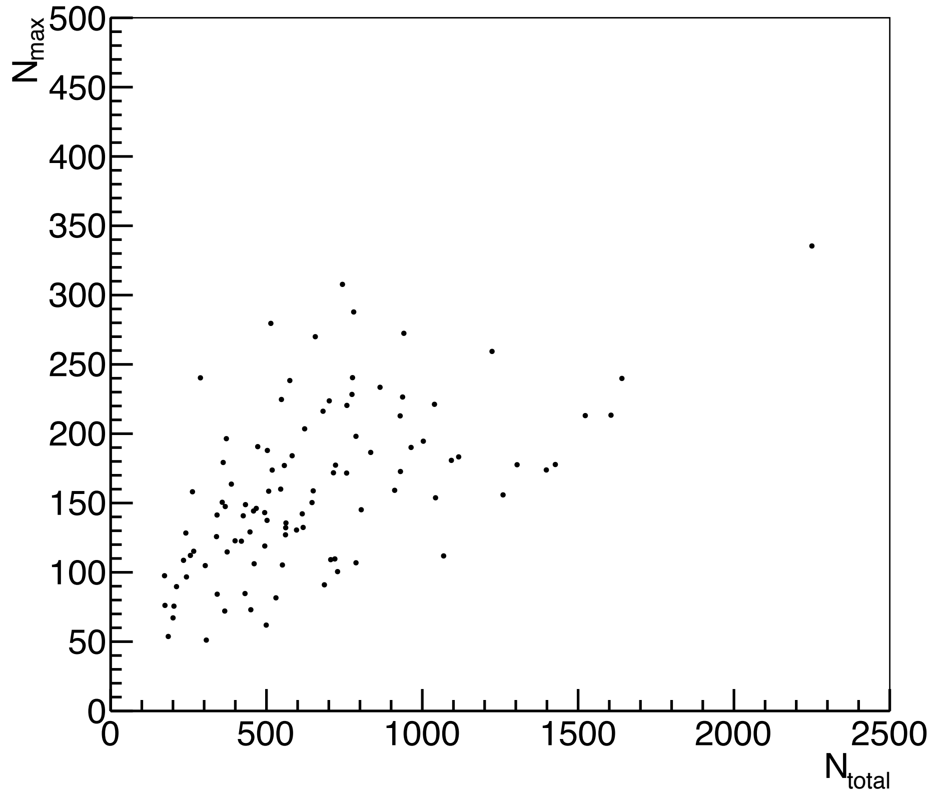

Figure 21: Correlation between the total number of hits in the shower N_{tot} and the maximum number of hits in one layer N_{max}

Figure 21 shows a strong correlation between the total number of hits in the shower and the maximum number of hits in one layer. This is as expected because the layer with the maximum number of hits is a part of the total and therefore contributes to the total number of hits.

7.4.2 Length vs total

The next correlation that is interesting is the one between the length of the shower and the total number of hits within the shower. This one is interesting because it can find showers that are short but have a high number of hits (all the energy of an incoming particle is deposited in a few layers).

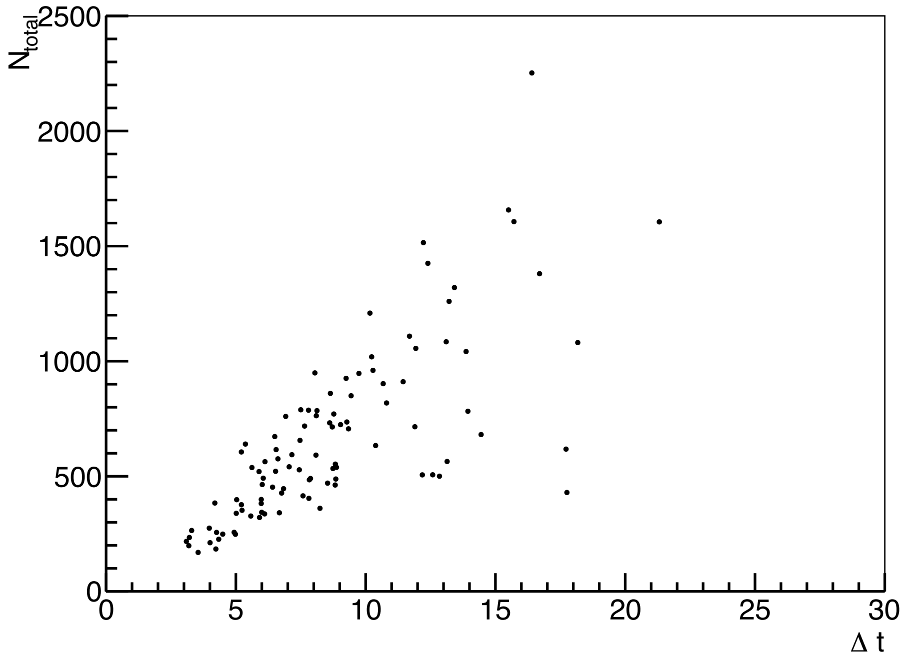

Figure 22: Correlation between the length of the shower Δt and the total number of hits within the shower N_{tot}

Figure 22 shows a strong correlation between the length of the shower and the total hits within the shower this is expected. But the interesting results from the figure is the absence of events in the top left corner. This indicates that there are no short showers with a lot of hits per layer. The other interesting result is that there are some events in the bottom right corner which indicates long showers without a high number of hits in the layers.

7.4.3 Length vs max

The correlation between length of the shower and the maximum number of hits in one layer is also interesting because there is no direct correlation between the two quantities.

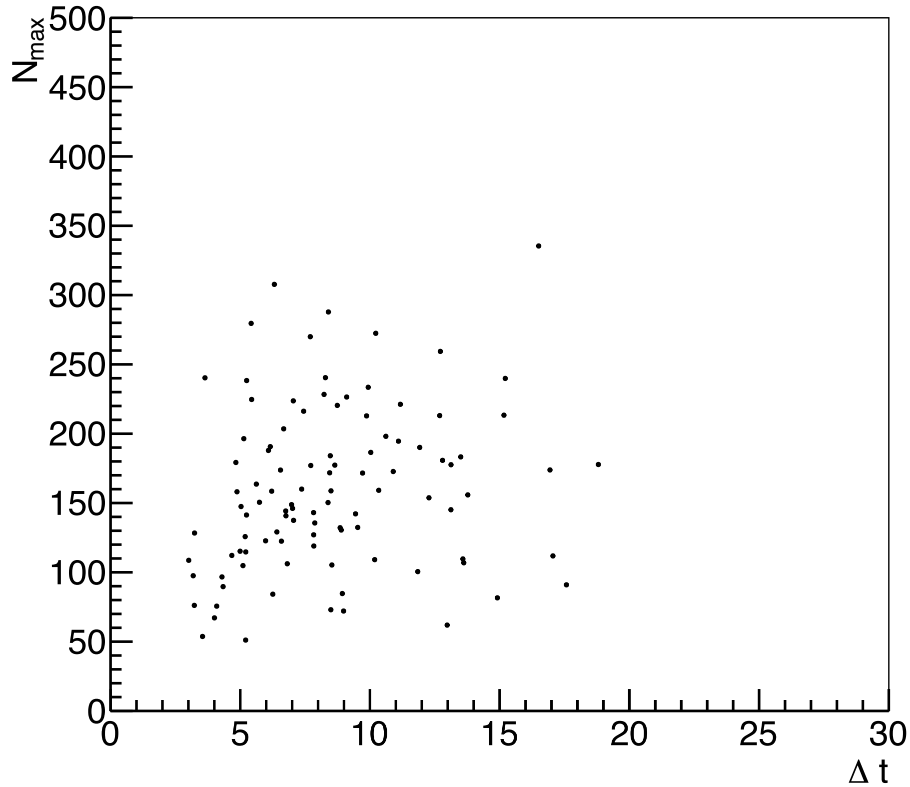

Figure 23: Correlation between length of the shower Δt and maximum number of hits in one layer N_{max}

Figure 23 shows a random distribution of the correlation between the length of the shower and the maximum number of hits in one layer as expected for two quantities that are not directly correlated. But with the difference that there are events that have a short length of the shower and have a high number of maximum hits in one layer. This may indicate that there is a type of hadronic shower at which a large part of the created particles are stopped in one layer. The events in the bottom right corner indicate that there are also showers that are relatively long and do not have high peaks in their longitudinal profile.

8 Discussion and further research

The goal of this thesis was to distinguish between the different hadronc showers. This is done by calculating characteristics from the experimental data and compare those characteristics with the simulated data.

8.1 Discussion

8.1.1 Statistics

One of the biggest challenges from this project was the lack of data. With more statistic, it would be possible to better test the simulation. The simple way to get better statistic would be to measure for a longer time. The other way would improve the data taking time if that happens less event will be thrown out by the past and future protection and it will measure more events.

8.1.2 Simulation

Due to the limited time, a good analysis of the best charge sharing threshold was not possible. This is, however, essential if the simulated data is to be compared to the experimental data. So one of the recommendations for further research should be to set up a protocol to find the right threshold value for different energies. If this is done all the analysis macro's developed for this research can be used without complicated adjustments. The hit distributions shown in figure 12 and 13 are significantly different from the experimental hit distributions (figures 9 and 10). The differences are clearest in the place of the peak and the events with more than 4000 hits. It looks like the x-axis is scaled by a factor of two compared to the experimental plots. This is hard to physically explain and could come from a bug in the simulation software. This bug should be fixed in order to make a useful analysis of the simulated data.

8.2 Characteristics

The approach to study the showers event by event is a good method to find get an inside in the different types of hadronic showers. The only downside of this approach is that the definitions are arbitrary. It would be interesting for future studies to test multiple different definitions of start and end point and analyse the different results. Another method to study the different events is by tracking the incoming particle and find the exact place (x,y and z-coordinates) in the detector where the first reaction takes place. With the information of this points the produced particles monitored and predictions can be made which type of hadronic reaction incoming particle had with the absorber. The physical size of the detector is also a challenge in this research because there is some leakage at the sides of the detector. But it is very challenging to develop a wider detector because of the size of the readout electronics and the data taking would be challenging (because of the great number of individual pixels).

8.3 Conclusion

The goal of this research was to analyse the different hadronic showers and develop a way to distinguish them. This is not achieved within this research, three experimental reasons are mentioned above. Another physical reason that the goal is not achieved is the fact that hadronic showers have a more complicated structure than was expected at the beginning of the research.

References

[1] M. Henley & A. Garcia ”Subatomic Physics” Third Edition, World Scientific 2007.

[2] M. Reicher, ”Digital Calorimetry Using Pixel Sensors” PhD thesis, Utrecht University,2016.

[3] Bichsel H., Groom D.E., Klein S.R.April 2002 *PASSAGE OF PARTICLES THROUGH MATTER*.

[4] ”PhotoMultiplierTubeAndScintillator”, https://upload.wikimedia.org/wikipedia/commons/5/5f/PhotoMultiplierTubeAndScintillator.jpg

[5] ”The Proton Synchrotron” https://home.cern/about/accelerators/proton-synchrotron

[6] J. Bloemkolk,”Analysis of the beam test data collected at CERN Proton Synchroton Facility”, Bachelor’s thesis, Utrecht University,2015.

[7] Particle Data Group, Atomic and Nuclear Properties of Materials, http://www-pdg.lbl.gov/2016/AtomicNuclearProperties/index.html

[8] R. K.Bock, Hadronic Shower”. http://rd11.web.cern.ch/RD11/rkb/PH14pp/node80.html

[9] S. Tavernier,Experimental Techniques in Nuclear and Particle Physics. http://www.springer.com/gp/book/9783642008283

[10] G. Nooren, Private communication, 2017

[11] T. van der Brink, Private communication, 2017

Appendices

A Layout of the detector

readout			layer		radiation thickness	interaction depth	
chip#	slot	box		Z [mm]	t [X_0]	p [λ] pion	p [λ] proton
3	1	0	0	1,9			
0	1	0	0	2,1			
1	1	0	0	2,1			
2	1	0	0	1,9	0,0		
47	12	0	1	5,9			
44	12	0	1	6,0			
45	12	0	1	6,0			
46	12	0	1	5,9	1,0	0,0	0,1
51	1	1	2	9,8			
48	1	1	2	10,0			
49	1	1	2	10,0			
50	1	1	2	9,8	2,0	0,1	0,1
95	12	1	3	13,8			
92	12	1	3	13,9			
93	12	1	3	13,9			
94	12	1	3	13,8	2,9	0,1	0,1
7	2	0	4	17,7			
4	2	0	4	17,9			
5	2	0	4	17,9			
6	2	0	4	17,7	3,9	0,1	0,2
43	11	0	5	21,8			
40	11	0	5	21,9			
41	11	0	5	21,9			
42	11	0	5	21,8	4,9	0,2	0,2
55	2	1	6	25,7			
52	2	1	6	25,9			
53	2	1	6	25,9			
54	2	1	6	25,7	5,9	0,2	0,3
91	11	1	7	29,7			
88	11	1	7	29,9			
89	11	1	7	29,9			
90	11	1	7	29,7	6,8	0,2	0,3
11	3	0	8	33,7			
8	3	0	8	33,9			

9	3	0	8	33,9			
10	3	0	8	33,7	7,8	0,2	0,4
39	10	0	9	37,7			
36	10	0	9	37,9			
37	10	0	9	37,9			
38	10	0	9	37,7	8,8	0,3	0,4
59	3	1	10	41,7			
56	3	1	10	41,9			
57	3	1	10	41,9			
58	3	1	10	41,7	9,8	0,3	0,5
87	10	1	11	45,7			
84	10	1	11	45,8			
85	10	1	11	45,8			
86	10	1	11	45,7	10,7	0,3	0,5
15	4	0	12	49,7			
12	4	0	12	49,8			
13	4	0	12	49,8			
14	4	0	12	49,7	11,7	0,4	0,5
35	9	0	13	53,7			
32	9	0	13	53,9			
33	9	0	13	53,9			
34	9	0	13	53,7	12,7	0,4	0,6
63	4	1	14	57,7			
60	4	1	14	57,8			
61	4	1	14	57,8			
62	4	1	14	57,7	13,7	0,4	0,6
83	9	1	15	61,6			
80	9	1	15	61,8			
81	9	1	15	61,8			
82	9	1	15	61,6	14,6	0,4	0,7
19	5	0	16	65,6			
16	5	0	16	65,8			
17	5	0	16	65,8			
18	5	0	16	65,6	15,6	0,5	0,7
31	8	0	17	69,6			
28	8	0	17	69,8			
29	8	0	17	69,8			
30	8	0	17	69,6	16,6	0,5	0,8
67	5	1	18	73,7			
64	5	1	18	73,7			

65	5	1	18	73,7			
66	5	1	18	73,7	17,6	0,5	0,8
79	8	1	19=0	77,6			
76	8	1	19=0	77,8			
77	8	1	19=0	77,8			
78	8	1	19=0	77,6	18,5	0,6	0,9
23	6	0	20	81,7			
20	6	0	20	81,8			
21	6	0	20	81,8			
22	6	0	20	81,7	19,5	0,6	0,9
27	7	0	21=0	85,7			
24	7	0	21=0	85,9			
25	7	0	21=0	85,9			
26	7	0	21=0	85,7	20,5	0,6	0,9
71	6	1	22	109,9			
68	6	1	22	110,0			
69	6	1	22	110,0			
70	6	1	22	109,9	26,7	0,8	1,2
75	7	1	23	113,9			
72	7	1	23	113,9			
73	7	1	23	113,9			
74	7	1	23	113,9	27,6	0,9	1,2
27	7	0	21=24	315,9			
24	7	0	21=24	315,9			
25	7	0	21=24	315,9			
26	7	0	21=24	315,9	42,0	1,9	2,2
79	8	1	19=25	519,9			
76	8	1	19=25	519,9			
77	8	1	19=25	519,9			
78	8	1	19=25	519,9	55,9	2,9	3,2

B Left out plots

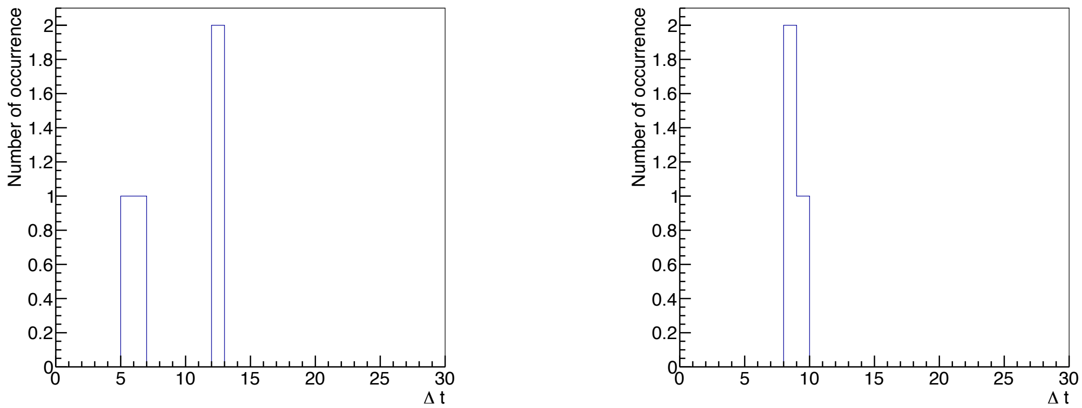

Figure 24: length of pions left 8 GeV/c and right 10 GeV/c

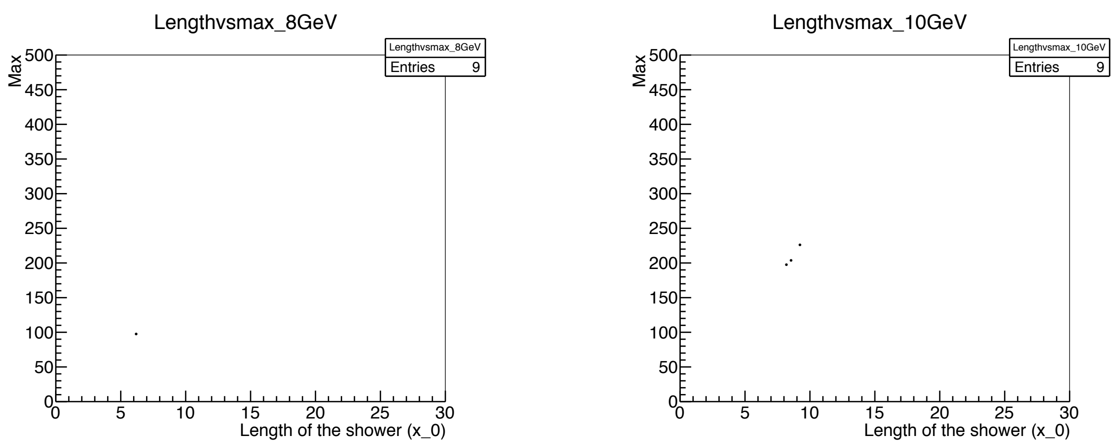

Figure 25: Length vs max of pions left 8 GeV/c and right 10 GeV/c

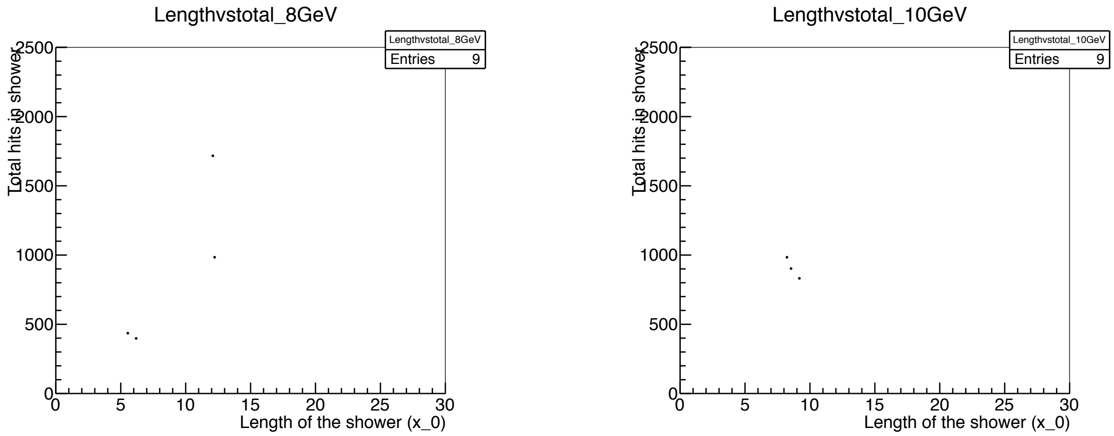

Figure 26: Length vs total of pions left 8 GeV/c and right 10 GeV/c

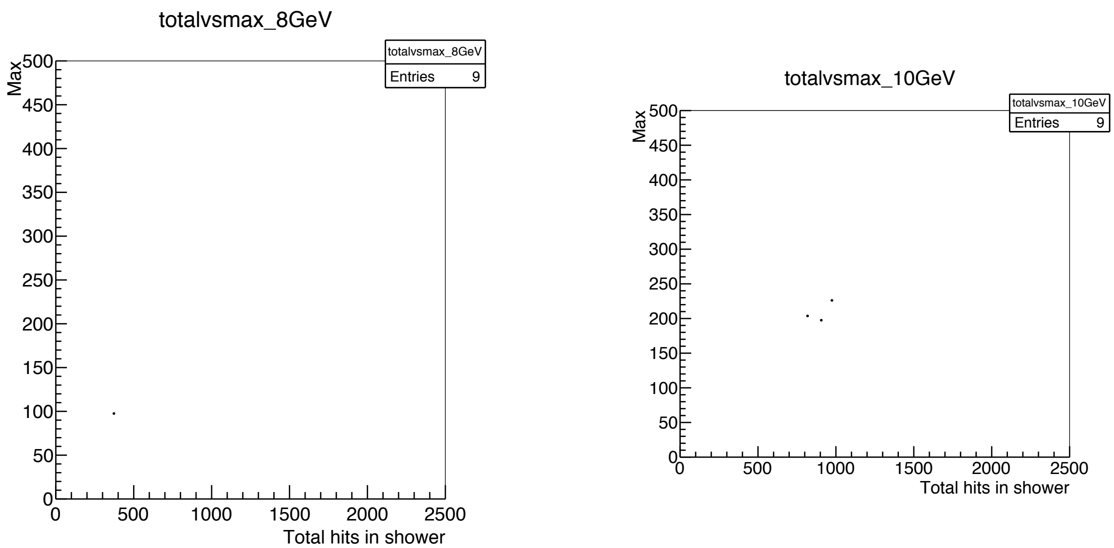

Figure 27: total vs max of pions left 8 GeV/c and right 10 GeV/c

C Appendix simulation variables and geometry of the virtual detector.

Table 7: Variables used in the simulation

Variables	value
Number of events	1000
Number of particles	1
Particle type	2212 for protons and 211 for pions
X coordinate incoming particles	Flat distribution from -0.5 to 0.5
Y coordinate incoming particles	Flat distribution from -0.5 to 0.5
Z coordinate incoming particles	Exact position -90
t	1
Energy of the particles	10 or 8
phi orientation angle	exact 0
theta orientation angle	exact 0
polx	exact 1
poly	exact 0
polz	exact 0

Table 8: Materials with properties

medium	density	isvol	ifield	fieldm	tmaxfd	stemax	deemax	epsil	stmin	components
silicon	2.3290	0	0	0	0.1	0.00000001	0.00000001	0.0000	0.00000	SI 1
tungsten	19.3	0	0	0	10	0.1	0.1	0.1	0.1	W 1
aluminum	2.70	0	0	0	10	0.1	0.1	0.1	0.1	AL 1
rvs	8.03	0	0	0	10	0.1	0.1	0.1	0.1	C 0.01 NI 0.075 Cr 0.175 Fe 0.74
circuitthick	1.85	0	0	0	10	0.1	0.1	0.1	0.01	AU 0.03 NI 0.04 CU 0.3657 SI 0.0513 O 0.1425 H 0.1995 CL 0.0057 C 0.1653
circuitthin	1.85	0	0	0	10	0.1	0.1	0.1	0.0001	AU 0.04 NI 0.06 CU 0.6426 SI 0.0234 O 0.065 H 0.091 CL 0.0026 C 0.0754
silverglue	5.25	0	0	0	10	0.1	0.1	0.1	0.0001	AG 1
vacuum	10^{-11}	0	0	0	10	1	0.1	0.0001	0.1	H 1
air	0.0012	0	0	0	10	1	0.1	0.0001	0.1	C 0.0001 N 0.7553 O 0.2318 AR 0.0128
sicintillator	1.03	0	0	0	10	1	0.1	0.1	0.1	H 0.085 C 0.915
copper	8.96	0	0	0	10	0.1	0.1	0.1	0.1	CU 1

The Parts of the detector.

Plastic scintlator

VOLUME p BOX 5.5 5.5 0.50 0 0 -23.3 sicintillator
VOLUME h BOX 2.0 0.5 0.25 0 0 -17.4 sicintillator
VOLUME v BOX 0.5 1.0 0.25 0 0 -16.6 sicintillator
VOLUME f BOX 2.0 2.0 0.50 0 0 -6.5 sicintillator
COMPOSITE scintilators
p 0 0 0 0 0 0 0
h 0 0 0 0 0 0 0
v 0 0 0 0 0 0 0
f 0 0 0 0 0 0 0

CIRCUITBOARDS

VOLUME circuitboard BOX 1.14 0.9805 0.008 1.14 0.9805 0.008 circuitthin
VOLUME underlayer BOX 1.0785 0.9805 0.00499 1.0785 0.9805 0.00499 silicon
VOLUME activelayer BOX 0.96 0.96 0.0010 0.96 0.96 0.0015 silicon
COMPOSITE chip underlayer 0 0 0 0 0 0 0
activelayer 0.06076 0.0364 0.01 0 0 0 0

CHIPBOXLEFT

VOLUME glue BOX 1.0785 0.9805 0.002 0 0 0.002 silverglue
VOLUME chipboxleft BOX 1.0785 0.9805 0.01 0 0 0.01 air
POSITIONIN chipboxleft glue 0 0 0 0 0 0 0
POSITIONIN chipboxleft chip -1.0785 -0.9805 0.004 0 0 0 0

CHIPBOXRIGHT

VOLUME chipboxright BOX 1.0785 0.9805 0.01 0 0 0.01 air
POSITIONIN chipboxright glue 0 0 0 0 0 0 0
POSITIONIN chipboxright chip -1.0785 -0.9805 0.004 0 0 0 0

ASSEMBLY LEFT

COMPOSITE assemblyleft glue 1.0115 0.9805 0 0 0 0 0
circuitboard -0.06576 0 0.004 0 0 0 0
chipboxleft 1.01274 0.9805 0.02 0 0 0 0

ASSEMBLY RIGHT

COMPOSITE assemblyright glue 1.0115 -0.9805 0 0 0 0 0
circuitboard -0.06576 -1.961 0.004 0 0 0 0
chipboxright 1.01274 -0.9805 0.02 0 0 0 0

ASSEMBLY(the gap)

VOLUME gluefilter BOX 0.9650 2.0 0.0035 0 0 0.0035 silverglue
VOLUME filler BOX 0.9650 2.0 0.015 0 0 0.015 tungsten
COMPOSITE miturefilter gluefilter 0 0 0 0 0 0 0
filler 0 0 0.007 0 0 0 0

VOLUME spacer BOX 1.45 0.20 0.04 0 0 0.04 rvs
VOLUME absorber BOX 2.50 2.50 0.0750 0 0 -0.0750 tungsten
COMPOSITE assembly assemblyleft 0 0 0 0 0 0 0
assemblyright 0 0 0 0 0 0 0
miturefilter -1.032 0 0 0 0 0 0
absorber 0.5 0 0 0 0 0 0

blocker
VOLUME blocker BOX 2.90 2.50 1.000 0 0 0 tungsten VOLUME window BOX 2.0 2.0 0.015 0 0 0 tungsten
VOLUME absorberAl BOX 2.50 2.50 0.075 0 0 -0.0750 aluminum
COMPOSITE assemblyfront assemblyleft 0 0 0 0 0 0 0
assemblyright 0 0 0 0 0 0 0
miturefilter -1.032 0 0 0 0 0 0
absorberAl 0.5 0 0 0 0 0 0

VOLUME unit BOX 3.1 2.8 0.195 0 0 0.045 air
POSITIONIN unit assembly 0 0 0 0 0 0 0
POSITIONIN unit assembly 0 0 0.09 0 180 180 1

VOLUME unitfront BOX 3.1 2.8 0.195 0 0 0.045 air
POSITIONIN unitfront assemblyfront 0 0 0 0 0 0 0
POSITIONIN unitfront assembly 0 0 0.09 0 180 180 0